Title
A p INTERACTIONS IN MOMENTUM RANGE 300 TO 1500 MeV/c

Authors
Kadyk, J.A.
Alexander, G.
Chan, J.H.
et al.

Publication Date
1970-11-01

Submitted to Nuclear Physics B

UCRL-20074
Preprint

c. 2

Λp INTERACTIONS IN MOMENTUM RANGE 300 TO 1500 MeV/c

J. A. Kadyk, G. Alexander, J. H. Chan
P. Gaposchkin, and G. H. Trilling

November 1970

AEC Contract No. W-7405-eng-48

LAWRENCE RADIATION LABORATORY
UNIVERSITY of CALIFORNIA BERKELEY

DISCLAIMER

Λp INTERACTIONS IN MOMENTUM RANGE 300 TO 1500 MeV/c*

J. A. Kadyk, G. Alexander,† J. H. Chan, P. Gaposchkin, and G. H. Trilling

Department of Physics and Lawrence Radiation Laboratory
University of California, Berkeley, California 94720

November 4, 1970

Abstract: A sample of approximately 250 Λp interactions has been obtained in the Λ momentum range of about 300 to 1500 MeV/c. An enhanced Λ production rate was obtained by exposing an internally-mounted platinum target to the incident 1.5-GeV/c K^- beam. Cross sections and angular distributions are obtained for the reactions: $\Lambda p \to \Lambda p$, $\Lambda p \to \Sigma^0 p$ and $\Lambda p \to \Lambda p \pi^0$. In the elastic channel, no strong evidence is seen near the $\Sigma^0 p$ threshold for the presence of a $^3S_1$ resonance, which has been reported, although there is some evidence for a small enhancement in this mass region. There is evidence for the presence of P-waves and probably also D-waves above about 800 MeV/c, but not below this momentum.

1. INTRODUCTION

The elementary hyperon-nucleon interaction is difficult to study experimentally because of the relatively small probability that the short-lived hyperon will interact rather than decay. We present here results from an experiment [1-3] designed to increase the number of observable Λ-proton interactions by enhancing the rate of Λ production. This was done by using a platinum plate mounted inside the Lawrence Radiation Laboratory 25-inch hydrogen bubble chamber as a target for a separated K^- beam. Nearly 100,000 Λ decays have been observed in about 260,000 photographs, and the data discussed here come from about 250 fitted Λp interactions. For a summary of previous work see ref. [4].

---

*Work supported by the U. S. Atomic Energy Commission.

†Present address: Department of Physics, Tel-Aviv University, Tel-Aviv, Israel.

2. LAMBDA MOMENTUM AND PATH-LENGTH DISTRIBUTIONS

The momentum of the K^- beam striking the platinum target is 1.5 GeV/c, and the Λ particles emerging lie roughly in the momentum range 300 to 1500 MeV/c, with a nearly constant path-length distribution between 500 and 1200 MeV/c. Further details on the use of the platinum plate and its geometry may be found in Refs. [1-3]. The momentum and path-length distributions, derived from a sample of fitted Λ decays, are shown in figs. 1 and 2. Approximately 8% of the total number of Λ decays observed were measured, but all the film was scanned twice, and the decays observed were recorded for each scan.

3. Λp INTERACTIONS--SCANNING AND MEASURING CRITERIA

The Λp reactions which we have studied are

$$\Lambda p \rightarrow \Lambda p \; , \tag{1}$$

$$\Lambda p \rightarrow \Sigma^{0} p \; ; \tag{2}$$

$$\Lambda p \rightarrow \Lambda p \pi^{0} \; . \tag{3}$$

Two other reactions expected to occur in this momentum range, $\Lambda p \rightarrow \Sigma^{+} n$ and $\Lambda p \rightarrow \Lambda n \pi^{+}$, have, by virtue of charge independence, cross sections just twice those of (2) and (3) respectively. Two-pion production, whose threshold is about 1300 MeV/c, is not important in this experiment. Λ interactions (1), (2), and (3) are all identified by the observation of a Λ decay associated with a proton track originating inside the bubble chamber. Since all these reactions have the same topology, they are distinguished only by kinematic fitting.

The reactions (1), (2), (3) must of course satisfy the three-constraint fit, which tests that the decaying Λ^{0} originates at the assumed interaction point. Moreover, the elastic reaction must satisfy an additional constraint at the scattering vertex. Events which satisfy the 3C fit at the Λ decay vertex but fail the 1C at the interaction vertex are presumably examples of reaction (2) or (3), but no further information can be derived without knowledge of the incident Λ direction. In order to develop the additional information needed to separate (2) from (3) and to provide greater confidence in the validity of events that satisfy the 1C fit to (1), an approximate determination of possible origins for the incident Λ^o was made as follows. Such origins were assumed to be along the lines of interacting K^- beam particles just halfway through the platinum plate. Since the platinum was so placed as to permit measurement of incident K^- tracks upstream from the plate, it was straightforward to measure for each picture with an interaction candidate all K^- tracks whose subsequent interactions could be Λ^o origins. In this way, the two additional constraints provided by knowledge of the direction of the incident Λ^o were available to confirm fits for reaction (1) and distinguish between (2) and (3). Errors assigned to these Λ^o directions reflected properly the uncertainty as to the actual position of the K^- interaction within the platinum. Occasionally, Λ^o directions determined in this way are in error because of a scattering in the plate of either the incident K^- or the outgoing Λ^o. An estimate of the consequences of this effect can be derived from comparing fits of reaction (1) with and without the Λ^o origin information. Thus the fraction of elastic events that fit no origin in the plate and yet fit well without use of the incident Λ direction is about 15%. This fraction is used to correct for the number of unfittable events from reactions (2) and (3) for cross-section determination (see below). From the complete sample of 222 events within the fiducial volume region, only two events fit, within reasonable probability limits, more than one reaction.

Reactions (2) and (3) require an origin for the initial Λ particle in order to obtain a kinematic solution, and therefore the effects of errors in the assigned origin locations for these reactions were studied. Such origin displacements may occur either due to a Λ or K^- scattering inside the plate, or due to ignorance of the exact origin position along the K^- beam path. The latter difficulty was avoided by making a succession of fits to five equally spaced origins inside the plate, along the paths of the K^- beam tracks. The effect of scattering inside the plate was studied by examining the events of reaction (1) where an origin is not required for the fit. Using these events, the amount and distribution of origin scattering was determined, and these were used in a Monte Carlo analysis [5] to predict the effects upon reactions (2) and (3). It was found that the fraction of events expected to fail these reactions was 13% and 15%, respectively. From these results, an estimate can be made for the number of events having a good three-constraint fit to the Λ decay vertex, but lacking a fit for the interaction vertex; namely, there should be eight such events. The number of events actually found, after background subtraction, was 12. The difference between these numbers is not significant, indicating that about 95% of the interactions have been kinematically identified. For purposes of cross-section determination, the remaining 12 events have been apportioned to the reactions according to the predicted failure rate.

In order to assure a sample of high reliability, two completely independent scans were made of the entire film and several additional conditions were required: A fiducial volume restriction was imposed both on the primary interaction vertex and on the decay vertex of the Λ, and the recoil proton was required to have a length of at least 2 mm. In the analysis each event was weighted to take account of the Λ escape probability; and, for cross-section determinations, a correction was made for events lost because of the 2-mm recoil length cutoff. Scanning efficiencies were computed by correlating the results of the two scans.

In our energy region, Λ decays are readily distinguished from K^0 decays. Kinematic fitting provides unambiguous identification in almost all cases, and the bubble density of the positive secondary removes essentially all ambiguity. Furthermore, K^op interactions are readily recognized: If they lead to a K_1^o decay the interaction is identified by the decay (since Λp interactions produce a negligible number of $\overline{K^o}$ particles), and if they lead to a Λ^o, the accompanying recoil track is a pion instead of a proton and hence recognizable by bubble density. Thus K^op interactions do not significantly contaminate our data sample.

4. RESULTS

4.1. Cross Sections

Channel cross sections are determined essentially by the ratio of the number of observed interactions to the Λ path length, as a function of Λ momentum. The distributions of these quantities are shown in figs. 1 and 2, and the cross sections derived from them are shown in fig. 3 as well as in table 1. Appropriate correction has been made for scanning efficiency as well as for the loss of a small number of inelastic events by scattering of the K^- or Λ within the platinum plate, as discussed in sect. 3. Figure 3d shows the total Λp cross section from 300 to 1500 MeV/c obtained by adding $\sigma(\Lambda p) + 3\sigma(\Sigma^o p) + 3\sigma(\Lambda\pi^o p)$.

For Λp elastic scattering, fig. 3a shows that the cross section has dropped to about 10 mb at 400 to 500 MeV/c, and seems to remain flat except for a rise in the region of the ΣN threshold. Both a Λp resonance and a Σp threshold cusp have been discussed in this region (at 620 and about 640 MeV/c respectively) and it is of interest to see whether the data support such behavior. Although both effects may reach the s-wave unitarity limit of about 50 mb for the $^3S_1$ state, a narrow width is expected for each, if it exists, so that only a small increase in the event population will be observed. If one assumes that a $^3S_1$ Λp resonance does exist, and little or no cusp occurs, then an upper limit to the resonance width may be calculated. The present data, taken from the momentum bin 600 to 700 MeV/c, yield an upper limit, with 90% confidence, of $\Gamma < 3.5$ MeV. Of course, the presence of a cusp may be responsible for some or all of the small rise observed.

The cross sections for the inelastic reactions (2) and (3) are shown in figs. 3b and 3c. The $\Sigma^0 p$ reaction proceeds strongly near threshold, but then diminishes quickly at higher momenta. A simple calculation shows that except just above threshold the Σ-nucleon cross section is well above the s-wave unitarity limit, implying a strong contribution from higher waves. Indeed, as will be seen from the angular distributions, there is strong evidence for higher waves above about 800 MeV/c.

4.2. Angular Distributions

The angular distribution in the elastic scattering channel is shown in figs. 4a and 4b for momenta below and above 800 MeV/c, respectively. The results of fitting these distributions to Legendre polynomials are given in table 2. At the higher momenta, there is strong evidence for the presence of p wave, and a fairly clear indication that d wave also occurs, while s wave suffices for a good fit at the lower momenta. The amount of s, p, and d waves is sufficient to explain the total cross section above 800 MeV/c.

Some deviation from isotropy can be observed in the $\Sigma^0 p$ and $\Lambda p \pi^0$ distributions, shown in figs. 4c and 4d, and in each there is some indication of forward peaking.

An examination was made for possible Λ polarization, either in the Λ beam or after interaction, and no significant effect was observed in any reaction. Of course in the $\Sigma^0 p$ case, since only 1/3 of the Σ^0 polarization is transferred to the Λ, no significant effect could be expected. (For all angular distributions the angle plotted is taken between the directions of incoming and outgoing hyperons in their c.m. system.)

We wish to thank Glenn Eckman and members of the crew of the 25-inch bubble chamber for their assistance in design and installation of the movable platinum plate, as well as members of the Bevatron operating staff for their support in running this experiment.

REFERENCES

[1] J. A. Kadyk, G. H. Trilling, G. Alexander, and P. J. Gaposchkin, Bull. Am. Phys. Soc. 14 (1969) 591.

[2] J. A. Kadyk, G. H. Trilling, G. Alexander, and P. J. Gaposchkin, Proc. Int. Conf. on Hypernuclear Physics, Argonne National Laboratory, Argonne, Illinois, May 5-7, 1969, p. 852.

[3] G. H. Trilling, J. A. Kadyk, G. Alexander, and P. J. Gaposchkin, Bull. Am. Phys. Soc. 14 (1969) 840.

[4] G. Alexander, O. Benary, U. Karshon, and U. Maor, Nucl. Phys. B10 (1969) 554.

[5] E. R. Burns, D. Drijard, and Y. Oren, Monte Carlo Program PHONY, Lawrence Radiation Laboratory Trilling-Goldhaber Technical Note TN-143, April 1968.

Table 1. Cross-section determinations.

Momentum interval (MeV/c)	Λ path length (m/100 MeV/c)	No. events $\Lambda p \to \Lambda p$ (weighted)	$\sigma(\Lambda p \to \Lambda p)$ (mb)	No. events $\Lambda p \to \Sigma^0 p$ (weighted)	$\sigma(\Lambda p \to \Sigma^0 p)$ (mb)	No. events $\Lambda p \to \Lambda p \pi^0$ (weighted)	$\sigma(\Lambda p \to \Lambda p \pi^0)$ (mb)	$\sigma_{total}(\Lambda p)$ (mb)
0-100	0	0	0					
100-200	15	0	0					
200-300	122	7.2	26.0					24±5
300-400	301	16.3	23.9					
400-500	469	9.5	8.9					9.0±2
500-600	543	11.2	9.1					
600-700	604	22.9	16.7	2.0	2.8			25±7
700-800	625	15.2	10.7	9.3	7.5			33±8
800-900	582	13.5	10.2	12.4	10.7			42±9
900-1000	603	12.2	8.9	6.0	5.0			24±7
1000-1100	532	21.9	18.1	4.0	3.8	1.0	1.6	28±6
1100-1200	454	7.1	6.9	3.0	3.3	2.0		
1200-1300	428	7.3	7.5	3.8	4.4	2.1	3.6	34±7
1300-1400	347	12.9	16.4	2.0	2.9	3.2		
1400-1500	301	7.8	11.4	1.0	1.7	2.0	3.0	30±8
1500-1600	254	7.7	13.3	2.1	4.1	1.2		
1600-1700	162	4.1	11.1	0	4.8	1.0	5.8	45±14
1700-1800	119	4.2	15.5	2.0		2.1		
1800-1900	68	2.1	13.6	1.6		0	5.7	
1900-2000	24	1.1	20.3	0		1.0		
Totals	6554	184.4 (175 unweighted)		49.3 (46 unweighted)		15.7 (15 unweighted)		

Table 2
Legendre polynomial fits to angular distributions.

Reaction	No. of events	Order of fit	A_1/A_0	A_2/A_0	A_3/A_0	χ^2	Degrees of freedom
$\Lambda p \to \Lambda p$	80	0	-	-	-	3.2	4
$(p_\Lambda)_{incident} < 800$ MeV/c		1	0.23±0.18	-	-	1.6	3
$\Lambda p \to \Lambda p$	101	0	-	-	-	24.8	4
$(p_\Lambda)_{incident} > 800$ MeV/c		1	0.67±0.1[illegible]	-	-	5.4	3
		2	0.70±0.16	0.26±0.23	-	4.2	2
		3	0.76±0.17	0.40±0.25	0.68±0.33	0.1	1
$\Lambda p \to \Sigma^o p$	48	0	-	-	-	5.9	4
(all momenta)		1	0.22±0.19	-	-	4.6	3
		2	0.25±0.27	0.73±0.35	-	0.3	2
		3	0.28±0.28	0.75±0.35	0.22±0.48	0.1	1
$\Lambda p \to \Lambda p \pi^o$	15	0	-	-	-	7.9	4
(all momenta)		1	0.59±0.3[illegible]	-	-	4.1	3
		2	0.58±0.50	1.00±0.74	-	2.3	2
		3	0.87±0.50	1.21±0.63	1.15±0.76	0.2	1

FIGURE CAPTIONS

Fig. 1. Momentum distribution for a sample of about 7700 free lambda decays.

Fig. 2. (a) Path-length distribution for lambdas, corresponding to fig. 1.

(b) Momentum distribution for 175 Λp elastic scatters.

(c) Momentum distribution for 46 events of the type $\Lambda p \rightarrow \Sigma^0 p$.

(d) Momentum distribution for 15 events of the type $\Lambda p \rightarrow \Lambda p \pi^0$.

Fig. 3. (a) Cross section for Λp elastic scatters.

(b) Cross section for the reaction $\Lambda p \rightarrow \Sigma^0 p$.

(c) Cross section for the reaction $\Lambda p \rightarrow \Lambda p \pi^0$.

(d) Total Λp cross section: $\sigma_{total} = \sigma(\Lambda p) + 3\sigma(\Sigma^0 p) + 3\sigma(\Lambda p \pi^0)$.

Fig. 4. (a) Angular distribution for elastic scatters, for incident Λ momentum less than 800 MeV/c.

(b) Angular distribution for elastic scatters, for incident Λ momentum greater than 800 MeV/c.

(c) Production angular distribution for the reaction $\Lambda p \rightarrow \Sigma^0 p$.

(d) Production angular distribution for the reaction $\Lambda p \rightarrow \Lambda p \pi^0$.

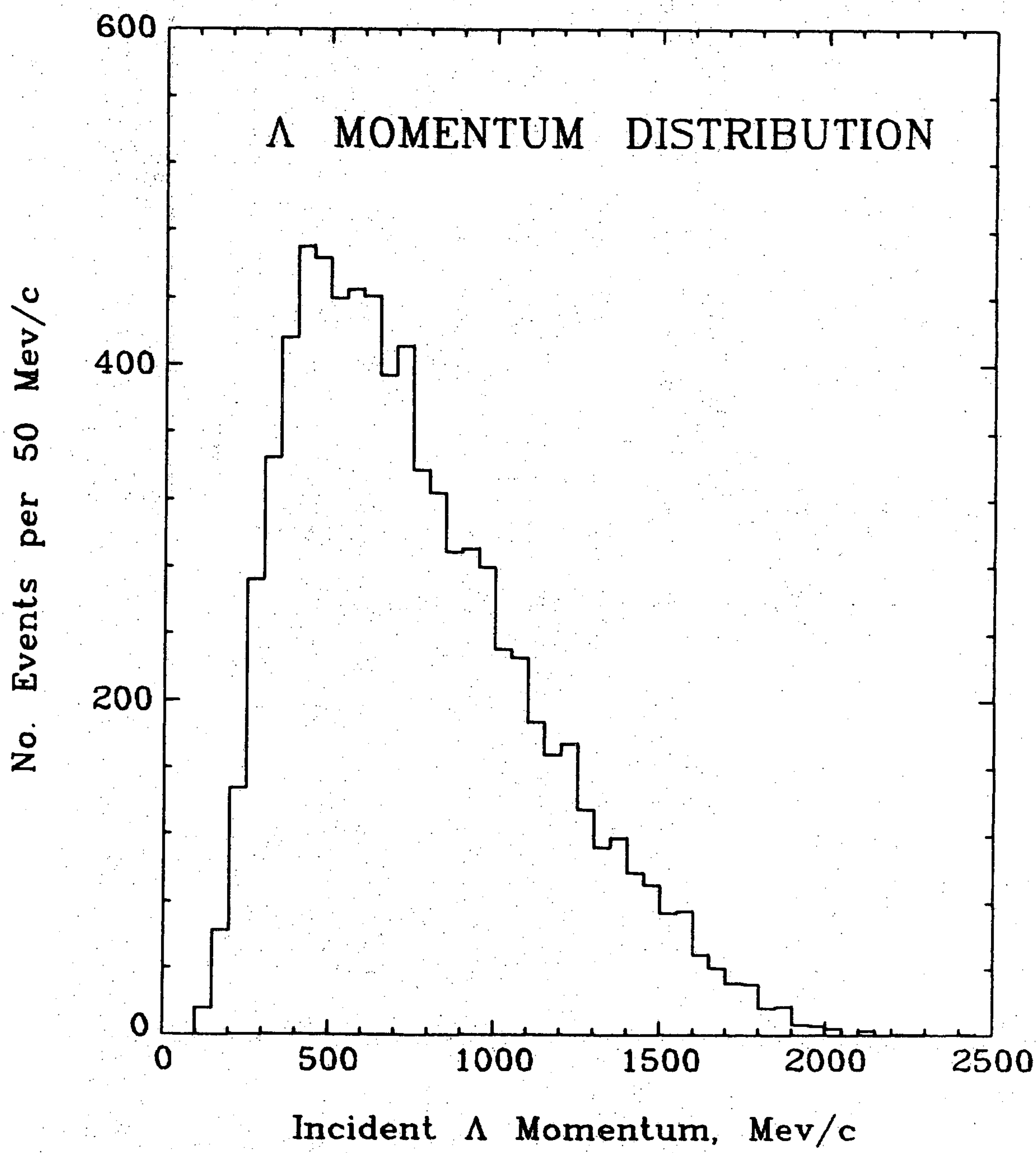

XBL 7011-6924

Fig. 1

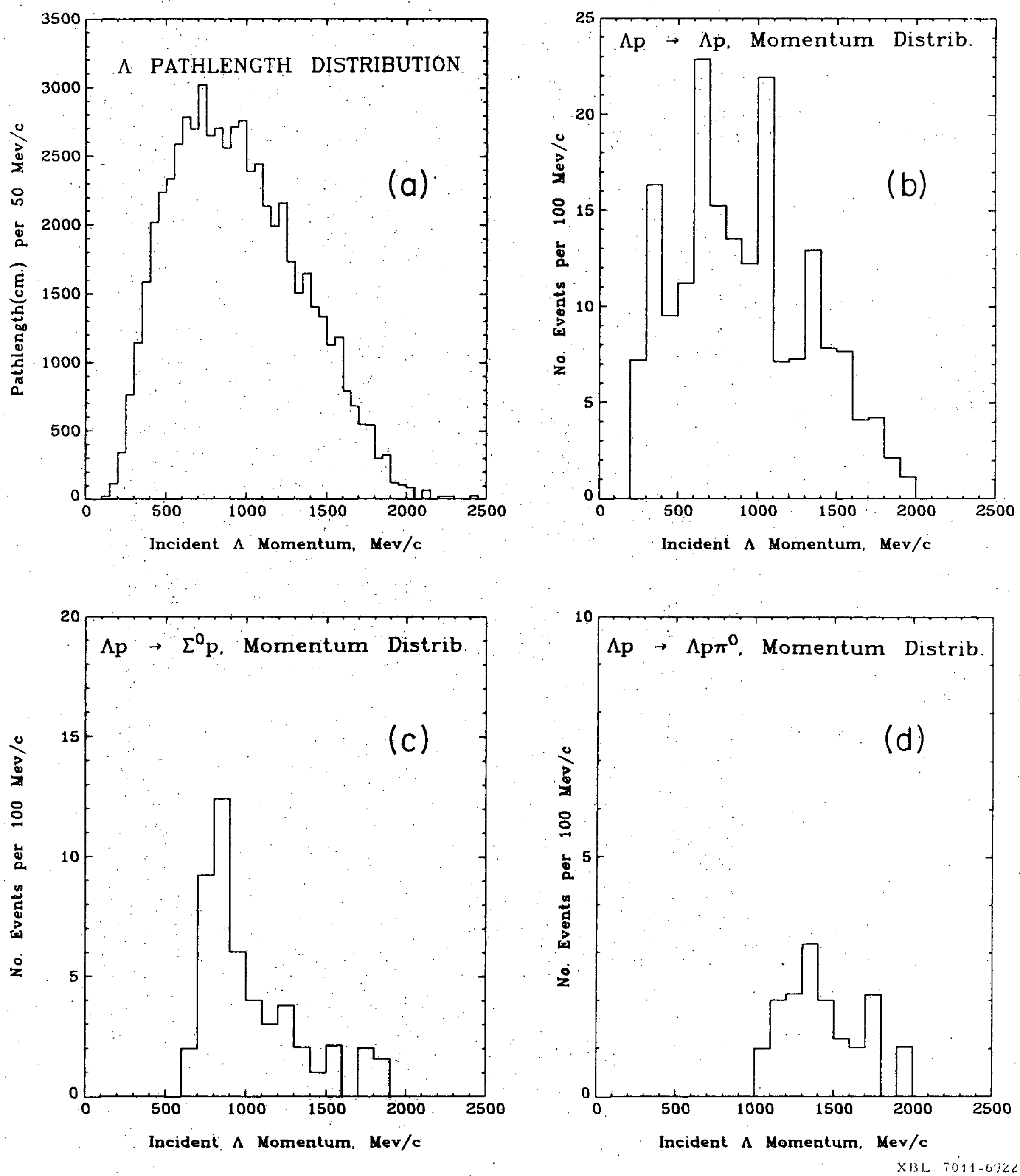
Λ PATHLENGTH DISTRIBUTION
(a)
Pathlength(cm.) per 50 Mev/c
Incident Λ Momentum, Mev/c
Λp → Λp, Momentum Distrib.
(b)
No. Events per 100 Mev/c
Incident Λ Momentum, Mev/c
Λp → Σ0p, Momentum Distrib.
(c)
No. Events per 100 Mev/c
Incident Λ Momentum, Mev/c
Λp → Λpπ0, Momentum Distrib.
(d)
No. Events per 100 Mev/c
Incident Λ Momentum, Mev/c
XBL 7011-6922

Fig. 2

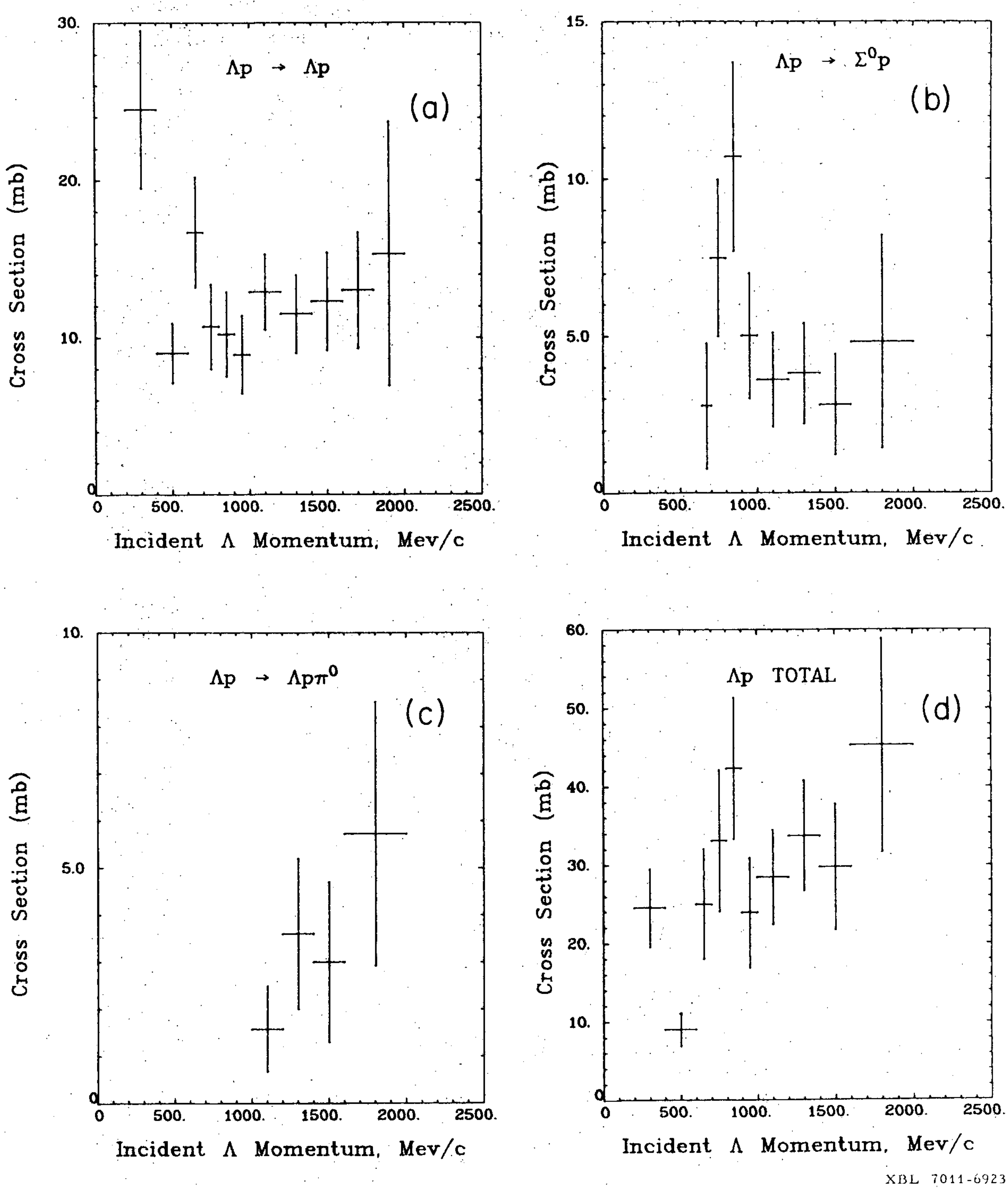
30.
20.
10.
0
Cross Section (mb)
$\Lambda p \rightarrow \Lambda p$
(a)
0 500. 1000. 1500. 2000. 2500.
Incident Λ Momentum, Mev/c
15.
10.
5.0
0
Cross Section (mb)
$\Lambda p \rightarrow \Sigma^0 p$
(b)
0 500. 1000. 1500. 2000. 2500.
Incident Λ Momentum, Mev/c
10.
5.0
0
Cross Section (mb)
$\Lambda p \rightarrow \Lambda p \pi^0$
(c)
0 500. 1000. 1500. 2000. 2500.
Incident Λ Momentum, Mev/c
60.
50.
40.
30.
20.
10.
0
Cross Section (mb)
Λp TOTAL
(d)
0 500. 1000. 1500. 2000. 2500.
Incident Λ Momentum, Mev/c
XBL 7011-6923

Fig. 3

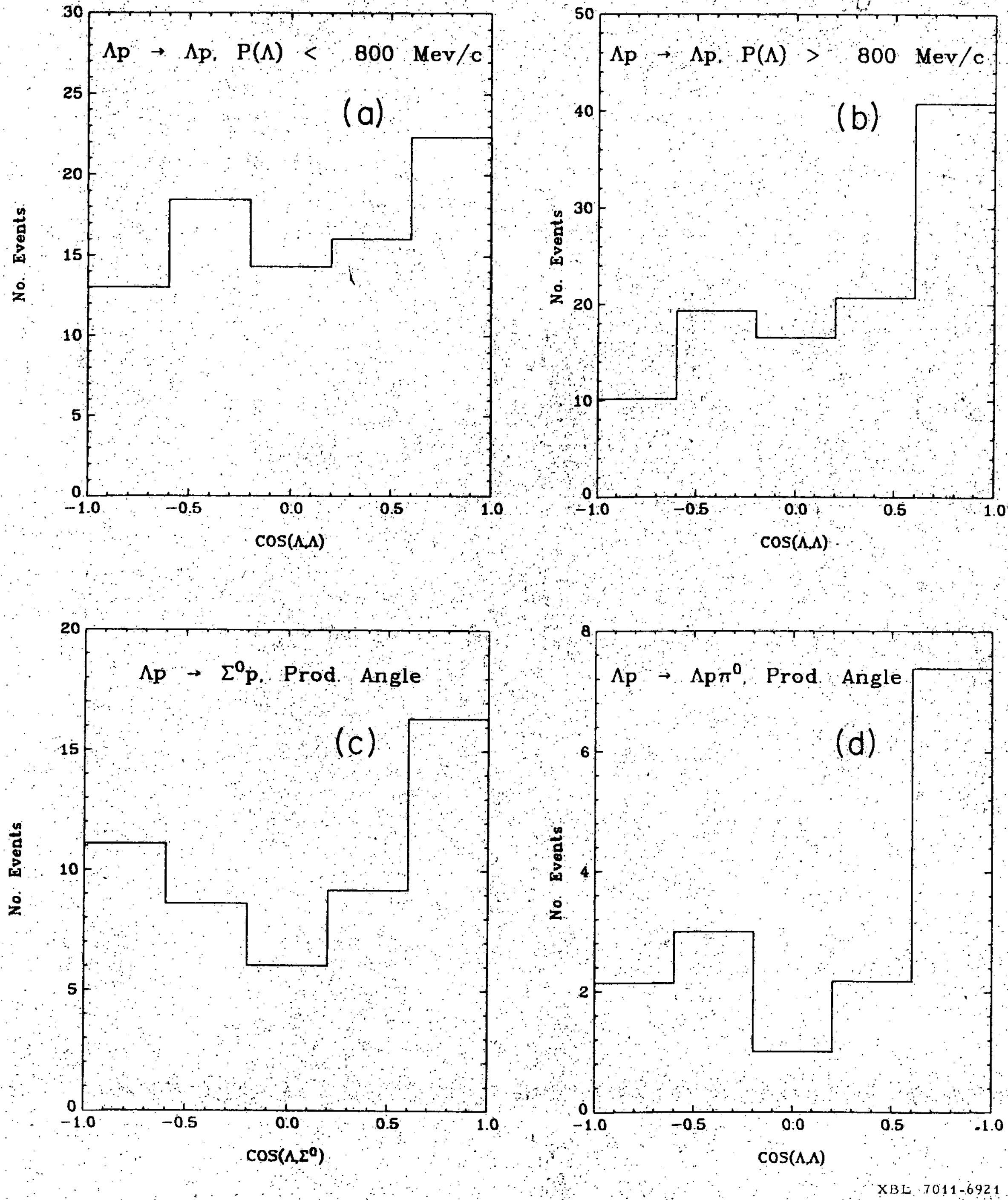

Λp → Λp, P(Λ) < 800 Mev/c
(a)
No. Events
COS(Λ,Λ)
Λp → Λp, P(Λ) > 800 Mev/c
(b)
No. Events
COS(Λ,Λ)
Λp → Σ⁰p, Prod Angle
(c)
No. Events
COS(Λ,Σ⁰)
Λp → Λpπ⁰, Prod Angle
(d)
No. Events
COS(Λ,Λ)
XBL 7011-6921

Fig. 4

TECHNICAL INFORMATION DIVISION
LAWRENCE RADIATION LABORATORY
UNIVERSITY OF CALIFORNIA
BERKELEY, CALIFORNIA 94720